Title

IMAGING WITH A MULTIPLANE MULTIWIRE PROPORTIONAL CHAMBER USING HEAVY ION BEAMS

Author

Chu, W.T.

Publication Date

1982-03-01

Peer reviewed

LBL-14143

IMAGING WITH A MULTIPLANE MULTIWIRE PROPORTIONAL CHAMBER USING HEAVY-ION BEAMS*

LBL--14143

DE82 014474

W. T. Chu, J. R. Alonso, and C. A. Tobias
Lawrence Berkeley Laboratory
University of California, Berkeley, California 94720

Abstract

A 16-plane multiwire proportional chamber has been developed to accurately map intensity profiles of heavy ion beams at the Bevalac. The imaging capability of the system has been tested for reconstruction of 3-dimensional representation of a canine thorax region using heavy ion beams.

Introduction

Accelerated heavy ions from the Bevalac are used for biomedical experiments. Often the radiation field areas are large, of diameters of 20 cm or larger, and the radiation intensities across the fields are desired to be uniform. To map the dose uniformity quickly, a 16-plane multiwire proportional chamber has been constructed and successfully used as a beam intensity monitoring device. It is named MEDUSA after MEdical Dose Uniformity SAmpler.

The 16 chamber planes, each of which has 64 parallel wires placed 4 mm apart, are stacked with their wire directions staggered in such a way that they cover the 180 degree space as shown in Fig. 1. When the heavy ions penetrate the chamber, the resulting ionization electrons are collected in each signal wire and stored in the integrating capacitor connected to the wire. The voltage on the capacitor is therefore proportional to the beam intensity over the area of a 4 mm-wide strip which is centered on the particular wire and extends midway toward the adjacent two wires. The voltage data collected on the 64 wires of a given chamber plane are the line integrals along the wires of the ionization resulting from the penetrating heavy ions. In other words, the data represent the one dimensional projection, along the direction of the wires, of the two-dimensional beam intensity profile. Based on the 16 projections, each at a different angle, the beam intensity profile is readily reconstructed. The reconstruction algorithm is based on the filtered back-projection technique.

CBB 783-3335

Fig. 1. MEDUSA.

The heavy ion beams at the Bevalac are pulsed at every 4 seconds, and MEDUSA is reset immediately prior to a beam pulse. At the end of each data collecting cycle, usually one or a few pulses, the capacitor voltages are sequentially sampled, digitized, and stored in a buffer memory under the control of an LSI-11 microprocessor. Upon command, the data in the buffer are serially transmitted to the host computer, a PDP 11/34 computer. The 1024 data points (16 planes of 64 wires) are used to reconstruct the beam profile,

*This work was supported by the Assistant Secretary for Health and Environmental Research Division of the U.S. Department of Energy under Contract No. W-7405-ENG-48 and by the National Institute of Health Grant CA15184.

*This work was supported by the Assistant Secretary for Health and Environmental Research Division of the U.S. Department of Energy under Contract No. DE-AC03-76SF00098, and by the National Institute of Health Grant CA15184.

MGW

usually in a 64 x 64 array with 4 mm pixel size. The reconstructed images are color coded according to the intensities and displayed on a RAMTEK 9351 system, which has a 512 x 512 pixel matrix with each pixel of 12-bit refreshable memory.

MEDUSA is used in the Biomedical facility of the Bevalac for routine beam intensity profile measurements and for new beam development. Imaging capability of MEDUSA using unmodified Bragg peak and spread Bragg peak have been also tested[1].

Beam Preparation for Imaging

Heterogenous 3-dimensional objects can be imaged using MEDUSA in the following way. If a heavy ion beam with a spread Bragg peak (spread by a specially designed filter, see below) is transmitted through a radiological object, MEDUSA positioned downstream of the object will detect the portion of the heavy ions in the peak that have excess energy after passing through the object. If the modified Bragg peak is shaped in such a way that the dose is a function of the penetration depth, then the measurement of the dose beyond an object represents the integral

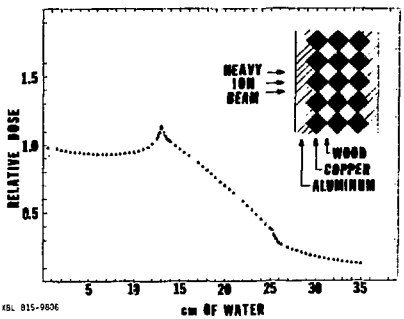

Fig. 2. The spread Bragg peak of a 670 MeV/amu neon-20 beam through a specially designed filter for imaging with MEDUSA.

stopping power of the object along the path of the beam. In other words, the reconstructed image of a 3-dimensional object using a heavy ion beam with a suitably modified Bragg peak is a 2-dimensional projection radiograph of the object, each pixel of which gives the integrated electron density seen by the beam particles arriving at the pixel's coordinates.

For imaging purpose, a special filter was constructed to produce a spread Bragg peak with a constant resolving power. It is assembled, as shown schematically in Fig. 2, using copper and wood rods with square cross-sections of 0.635 cm side, and aluminum plates with ridges. The monoenergetic heavy ions, distributed over the filter area, go through different amounts of absorbing materials, and emerge beyond it with their energies distributed as shown in Fig. 2. The filter modifies and spreads the Bragg peak of 670 MeV/amu neon-20 ions and produces a modified peak of 13 cm width of an approximately constant slope from 13 cm to 26 cm of water-equivalent penetration depth. Note that the finite dose beyond the distal peak at 26 cm is due to the nuclear fragmentations of the heavy ions in the intervening materials including the filter. The 670 MeV/amu neon-20 ion beam is laterally broadened by the first scatterer of 1.11 cm thick lead, positioned approximately 10 m from the object and MEDUSA, and is further broadened by the filter acting as the second scatterer, which is located about 6 m upstream of MEDUSA. The repetitious pattern of the filter is smeared by the multiple scattering of the ions in the filter itself, and no discernable beam structure due to it is detected at the location of MEDUSA. In summary, the first scatterer and the filter laterally broaden the heavy ion beam to a broad Gaussian intensity distribution over a circle of about 20 cm diameter at MEDUSA, and the filter spreads the Bragg peak to a width of approximately 13 cm. The overall range of the beam is adjusted by a variable-thickness water column introduced between the filter and the radiographic object.

Imaging with MEDUSA

A beagle under general anesthesia was propped up inside a plastic cylinder of 18 cm diameter, and placed immediately upstream of MEDUSA. The height was adjusted so that the general thorax area was in the beam. Approximately 2×10^4 particles/cm^2 of broadened and modified 670 MeV/amu neon-20 ions were used per exposure. To average out any pulse to pulse variation in the beam structure, the intensity of the extracted beam from the Bevalac was sufficiently lowered, so that an exposure spanned 5 Bevalac pulses (approximately 20 seconds). Four exposures were taken with the water column settings of 0, 4, 8, and 12 cm. Then the object was rotated by 11.25 degrees and four more exposures were taken. The process was repeated until 16 angular positions, each with 4 water column settings, were exposed. The beam profiles through the empty plastic cylinder were also taken for normalization purposes as the beam intensity profile was a broad Gaussian instead of a uniform flat distribution. For imaging an object with dimensions less than the spread Bragg peak width, 13 cm in this case, only one water column setting is needed for reconstruction; four water column settings were used for checking and calibration purposes. The reconstruction of 2-dimensional heavy-ion radiographs from these data are shown in Figure 3, which show the exposures of the canine thorax from 16 different angular directions.

If one takes one horizontal slice from each of the 16 2-dimensional projections in Figure 3 at a certain level, then a tomographic image may be reconstructed at that level. It is noted that

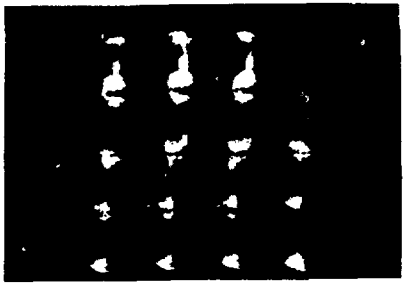

XBB 818-7850

Fig. 3. Two-dimensional projection heavy ion radiographs of a canine thorax from sixteen different angular directions.

XBB 818-7851

Fig. 4. Transverse tomographs of a canine thorax showing the heart, the two lungs, and the body contour.

the sensitive area of MEDUSA is a circle of 25.6 cm diameter, and the canine thorax is projected in its entirety in not all 16 views at high and low parts of the circle as seen in Figure 3. This affects the accuracy of the reconstructions discussed below.

Transverse tomographs of the canine thorax are shown in Figure 4. Out of the 64 possible slices, 12th to 45th slices are shown at every third slice. For the reconstruction, the data from Figure 3 are averaged over 3 slices, i.e., 12 mm thick slices, and the transverse tomographs were reconstructed again through the filtered back-projection technique. In Figure 4, the coutour of the body, the two lungs, the heart,

XBB 818-7852

Fig. 5. Sagittal tomographs of a canine thorax.

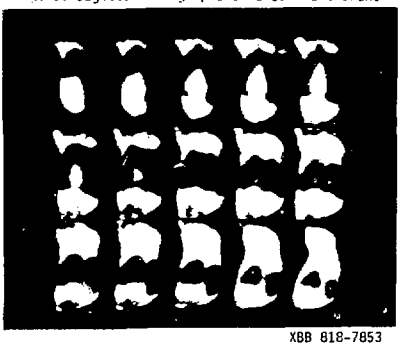

XBB 818-7853

Fig. 6. Coronal tomographs of a canine thorax.

and the spinal column are clearly visible.

Taking data from all 64 transverse sections, allowing the inaccuracies in top and bottom slices due to the limited view of MEDUSA as described above, the sagittal and coronal tomographs are reconstructed and shown in Figures 5 and 6, respectively. The sagittal slices in Figure 5 show 28th to 50th slice at every other slice, starting from left side and ending at right side of the dog. They clearly show the body contour, the lungs, the heart, and the diaphragm. The coronal slices in Figure 6 show 14th to 42nd slice at every other slice, starting at the frontal part and ending at the back of the dog. Again, they show the body contour, the lungs, the heart, and the diaphragm.

The uncertainties in the reconstructed electron density distribution stem mainly from two sources, namely, the statistics of the heavy

ions and the reconstruction based on data from a finite number of chamber planes and discrete spacings of signal wires of MEDUSA. The statistical error in the ionization due to the heavy ions in MEDUSA is analyzed in the following way. The dose-averaged linear energy transfer, <LET>, for neon at midpeak of a 14-cm spread Bragg peak (used for therapy) is

$\langle LET \rangle = 632\ MeV/cm^2/g$ in water.

On the other hand, the neon ions transmitted through the thick part of the object, those with 50 MeV/amu of kinetic energy possesses the energy loss,

$\Delta E/\Delta x = 1263.5\ MeV/cm^2/g$ in water.

Since the absorbed dose of 1 rad represents 6.25×10^7 MeV/g, 1 rad dose is given by 0.5×10^5 to 1.0×10^5 neon ions depending on the two values mentioned above. The average heavy ion flux used to expose MEDUSA was approximately 2×10^4 ions/cm^2. The dose per exposure in the middle of the object, where the ion flux is reduced to about one half of the incident beam, is estimated to be about 0.15 rad per exposure. Now each neon ion passing through 5 mm of argon gas (one plane of chamber) at STP, with the density of 1.66×10^{-3} g/cm^3 and mean excitation energy of 210 eV, has an energy loss of

$\langle \Delta E/\Delta x \rangle = 688 \pm 71$ keV, (FWHM = 141 keV).

Actually the distribution is not symmetric, with the skewness parameter K = 0.4938, but for our analysis it is assumed to be Gaussian. Since 2×10^4 ions/cm^2 is equal to 1.28×10^4 ions/(8 mm)^2, which represents the number of ions passing through a square made of two wire spacings, we take a half of the value, 0.64×10^4 ions/(8 mm)^2, to represent typical number of ions detected in MEDUSA per exposure. The percent statistical error in the measurement of ionization in an area incident by N particles is then,

$$\sigma_i = \frac{100}{\sqrt{N}} \left\{ 1 + \left(\frac{71}{688}\right)^2 \right\}^{1/2} \%$$

or $\sigma_i = 1.3\ \%$ for $N = 0.64 \times 10^4$ ions/(8 mm)^2 .

The uncertainty due to the reconstruction is estimated following the analysis by Huesman[2]. For MEDUSA, with 16 angular projections, each with 64 wires, and wire spacing of 4 mm, the uncertainty in the reconstructed electron density, σ_ρ, is related to σ_i as,

$$\sqrt{\langle \sigma_\rho^2 \rangle} = 2.4\ \langle \sigma_i \rangle ,$$

which is approximately 3%. In the above estimate, the reconstructed pixel size d = 8 mm (2 wire spacings), and the reconstructed image size D = 14 cm are used. Note that to obtain a tomographic image, two successive reconstructions are required in our system, and the uncertainties in electron densities are amplified accordingly to approximately 7%. In summary, MEDUSA can image a 3-dimensional object in pixel size of 8 mm with the reconstructed electron density to an accuracy of approximately 7% while exposing the object to about 2.4 rad of heavy ion radiation.

Conclusion

MEDUSA's imaging capability has been tested and demonstrated. Although it is a low spatial resolution device, it has the advantage of imaging the 3-dimensional object at once, instead of in a slice-by-slice way as in the case of CT scanners. Its resolution can be increased by a larger number of wire planes, finer wire spacings, and to a lesser extent by increased pressure of the chamber gas. Such a system, if used in conjunction with the heavy ion therapy program, will make it possible to assess the patient anatomy in relation to heavy ion beams with patient in the treatment position at the time of treatment.

Acknowledgements

We wish to thank R. Edwards and E. Stuart for mechanical design and fabrication of MEDUSA, D. Rondeau, R. Rozzano, and the LBL Real Time Systems Group for the design and construction of the electroncis of the system, R.P. Singh for software development, and the Biomedical facility and the Bevalac Operation staff. We also acknowledge our thanks to T. Budinger and B. Moyer for providing us the experimental animal and its care.

References

1. W.T. Chu, J.R. Alonso, and C.A. Tobias, "Heavy Ion Beam Studies and Imaging with a *Multiplane Multiwire Proportional Chamber*," IEEE Trans. Nucl. Sci. NS-28 (1981), 2198-2200.

2. R.H. Huesman, "The Effects of a Finite Number of Projection Angles and Finite Lateral Sampling of Projections on the Propagation of Statistical Errors in Transverse Section Reconstruction," Phys. Med. Biol. 22 (1977), 511-521.